Virchows Arch (1995) 427:91–99

ORIGINAL ARTICLE

Asami Kondo · Jiro Deguchi · Shigeru Okada

Renal cysts and associated renal tumours in male ddY mice injected with ferric nitrilotriacetate

Received: 4 October 1994 / Accepted: 27 March 1995

Abstract In experiments using ferric nitrilotriacetate (Fe-NTA) as a renal carcinogen, multiple renal cysts are often observed in addition to renal tumours. In the present study, we used 3-week-old male ddY mice and examined the relation between renal cysts and cancer development. Four months after the start of Fe-NTA administration, we observed cysts in the renal cortex in all Fe-NTA-treated mice, but not in Fe-free NTA-treated mice. Three types of cysts were observed, but only those which originated from the renal proximal tubules showed multilayered or papillary growth of cyst epithelial cells. Using histochemical staining, we found a cyst formation-tumour induction sequence, and the supposed cystic-papillary tumour induced by Fe-NTA was of proximal tubular cell origin. We also found that the minimum dose of Fe-NTA capable of inducing renal tumours in ddY mice was 10 mg of iron/kg/day, four times in 2 weeks.

Key words Ferric nitrilotriacetate · Renal proximal tubules · γ-glutamyltranspeptidase · Renal cysts · Renal tumours

Introduction

We have previously reported that parenteral administration of iron-chelated nitrilotriacetate (Fe-NTA) causes severe acute and subacute renal tubular necrosis through Fe-induced free radical chemistry [27] and induces renal tumour in rats and mice [11, 18, 26]. The reported method [11, 18, 26] for inducing renal tumours in rats and mice was to administer Fe-NTA intraperitoneally 6 days a week for 12 weeks. However, the minimum dose and time required for the induction of renal tumour by Fe-NTA was unclear.

During renal carcinogenesis in mice and rats, we noticed that almost all Fe-NTA-treated animals had many renal cysts of an undefined nature [18, 26] and that renal neoplasms developed among these cyst-bearing animals. According to our previous results, only the proximal tubules were the site of Fe-NTA-induced tubular necrosis at the acute and subacute stages [28, 35].

In the present study we tried to clarify the origin of the cysts and tumours and evaluated the relation of cysts and carcinogenesis by periodic acid-Schiff (PAS) stain, γ-glutamyltranspeptidase (γ-GTP), transforming growth factor-α (TGF-α), and lectin histochemistry. We also defined the minimum dose of Fe necessary to induce tumour transformation by modifying the total Fe dose in experimental groups.

A. Kondo · J. Deguchi · S. Okada (✉)
Department of Pathology, Okayama University Medical School, 2-5-1 Shikata-cho, Okayama 700, Japan

Materials and methods

Animals and treatments

Three-week-old male ddY mice (Shizuoka Laboratory Animal Center, Shizuoka, Japan) were used in all studies. All animals received humane care in compliance with "Guide for the Care and Use of Laboratory Animals" published by National Institutes of Health (publication number 86–23, revised 1985). They were maintained on a diet of commercial mouse chow (Funabashi F1, Chiba, Japan) and tap water ad libitum.

Table 1 shows the experimental groups and treatment. A total of 186 mice were used, which were divided into five groups. Experimental animals (from group 1 to group 4) were given Fe-NTA at a dose of 10 mg of iron/kg/day, intraperitoneally, twice a week for different lengths of time in different groups. In group 5, the NTA dose was equivalent to the NTA portion of the Fe-NTA injected in the group 4 animals. After the last injection, all animals were observed carefully. Animals for observation (not shown in the Table) were injected with Fe-NTA and were examined histologically 48 h after the last treatment and then every 2 months. All surviving animals in groups 1–5 were sacrificed under ether anaesthesia 12 months after the last treatment. Kidneys were horizontally sectioned, fixed in 10% phosphate-buffered formalin, and embedded in paraffin. They were sectioned at a thickness of 4 μm and stained with haematoxylin and eosin for routine examination. PAS stain, TGF-α immunohistochemistry [9, 38] and lectin histochemistry [16] were performed on paraffin sections. Frozen sections were prepared from a portion of the kidney at the same time for histochemistry of γ-GTP activity. The brush border of renal proximal tubules contains mucopolysaccharide which are stained red

purple by PAS stain [37] and have high γ-GTP activity [32, 34]. TGF-α is a good marker for collecting ducts and distal tubules in mice, but unlike rat and human renal cell tumours, mouse renal tumours are negative for TGF-α (unpublished personal experience). Other groups of animals were also used for histochemistry of lipid peroxidation in frozen sections not shown in the Table.

Chemicals

All reagents used were of the highest quality available. NTA disodium salt was purchased from Nacalai Tesque (Kyoto, Japan). All other reagents (unless specified) were purchased from Wako Pure Chemicals (Osaka, Japan). The monoclonal antibody against TGF-α was provided by Oncogene Science, (N.Y., USA). Four biotin-labelled lectins were provided by EY Laboratories (Calif., USA) and were used at the following dilution: wheat germ agglutinin (WGA): 10 μg/ml, soybean agglutinin (SBA): 10 μg/ml, peanut agglutinin (PNA): 10 μg/ml, *Dolichos biflorus* agglutinin (DBA): 10 μg/ml. Avidin-biotinylated peroxidase complex was provided by Vector Laboratories (Calif., USA). Fe-NTA was prepared by the method of Awai et al. [2]. Briefly, NTA disodium salt and ferric nitrate were separately dissolved in distilled water and the Fe solution was mixed with the NTA solution. The pH was adjusted to 7.2 with sodium bicarbonate. The molar ratio of Fe to NTA was 1:4, and the Fe concentration was 1 mg/ml.

Table 1 Experimental groups and treatments (*Fe-NTA* ferric nitrilotriacetate)

Group	Treatment	Fe dose (mg Fe/kg body weight)	Frequency of injection (per week)	Duration of treatments (weeks)
1	Fe-NTA[a)]	10	2	2
2	Fe-NTA[a)]	10	2	4
3	Fe-NTA[a)]	10	2	8
4	Fe-NTA[a)]	10	2	12
5	NTA[b)]	0	2	12

[a] The molar ratio of Fe to NTA was 1:4
[b] Dose equivalent to the NTA portion of Fe-NTA

Histochemical procedures

To observe the localization of Fe-NTA induced lipid peroxidation, histochemical detection was performed. Three-week-old male ddY mice were given one injection intraperitoneally with Fe-NTA at 10 mg Fe/kg, the same dosage as used in chronic experiments. The mice were killed 2 h after injection. The kidneys were quickly removed, frozen in liquid nitrogen, and processed for histochemical demonstration of lipid peroxidation, using cold Schiff's reagent [31].

TGF-α immunohistochemistry [9, 38] and lectin histochemistry [16] were performed according to previously reported methods and γ-GTP activity was observed histochemically in unfixed frozen section according to standard methods [20, 32].

Results

Animal data

Table 2 shows the incidence of animal deaths, simple or multilayered cysts and renal tumours 12 months after the last injection (13–15 months from the start of treatment). We found that the minimum injected dose of Fe-NTA capable of inducing renal tumours in ddY mice was 10 mg Fe/kg, 4 times in two weeks, as shown in Table 2. A higher incidence of renal tumours was found in groups 3 and 4 than in groups 1 and 2. Metastasis and tumour-related death were not found in any animals. One of the NTA-treated mice (in group 5) developed renal cysts but none of them had renal tumours. The microscopic appearance of renal tumours was cystic-papillary and solid. Cystic-papillary tumours were 73% of all tumours and solid tumours were 27%. There was no relation between histological type and the cumulative dose of Fe-NTA injected.

Histological and histochemical observations

Two hours after the Fe-NTA injection, 3-week-old male mice showed patchy Schiff positivity in the renal proxi-

Table 2 Indidence of deaths, cystic change and renal tumours in male ddY mice treated with Fe-NTA and NTA (animals examined for observation were omitted from this table)

Group	Number of mice			Number of mice with kidneys having:					
	Number of mice used	Number of deaths during		Number of mice surviving (%)	cystic change (%)[a)]	multilayered cystic change (%)[a)]	renal tumours (%)[a)]		
		treatment	observation				cystic-papillary	solid	total (%)[a)]
1	32	1	9	22 (69%)	22 (100%)	9 (41%)	2	1	3 (14%)
2	35	3	8	24 (69%)	24 (100%)	15 (63%)	1	2	3 (13%)
3	40	10	4	26 (65%)	26 (100%)	22 (85%)	6	1	7* (27%)
4	43	23	12	8 (19%)	8 (100%)	5 (63%)	2	0	2* (25%)
5	36	6	11	19 (53%)	1 (5%)	0 (0%)	0	0	0 (0%)

* Significantly different from NTA-treated mice by the χ^2-test, ($p<0.05$)
[a] The percentage means the incidence in the surviving mice

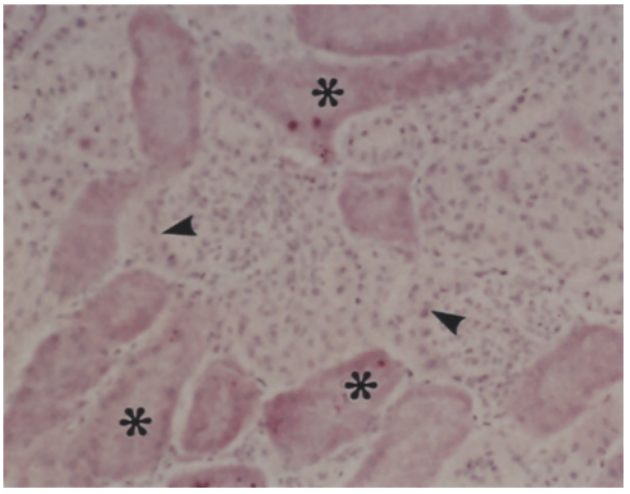

Fig. 1 Histochemical localization of lipid peroxidation of the kidney 2 h after ferric nitrilotriacetate (Fe-NTA) injection at 10 mg Fe/kg. Renal proximal tubules are positive for Schiff's stain *(asterisk)* but columnar cells of Bowman's capsule are all negative *(arrowhead).* (Cold Schiff's stain, ×200)

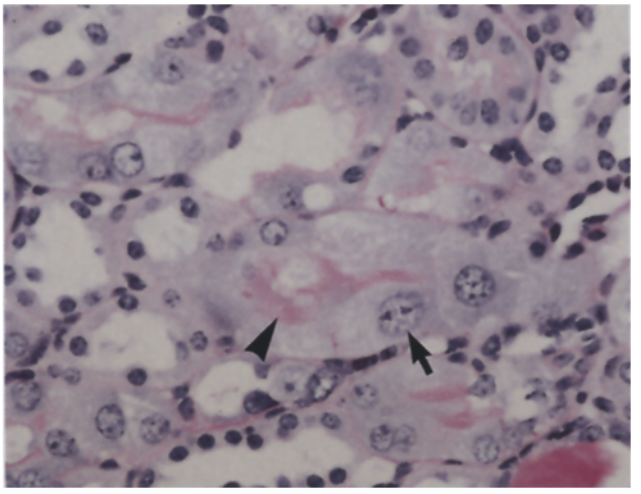

Fig. 2 Renal proximal tubules 48 h after the final Fe-NTA injection. Regenerative karyomegalic cells *(arrow)* have a brush border that is positive periodic acid-Schiff for PAS stain *(arrowhead).* (PAS, ×400)

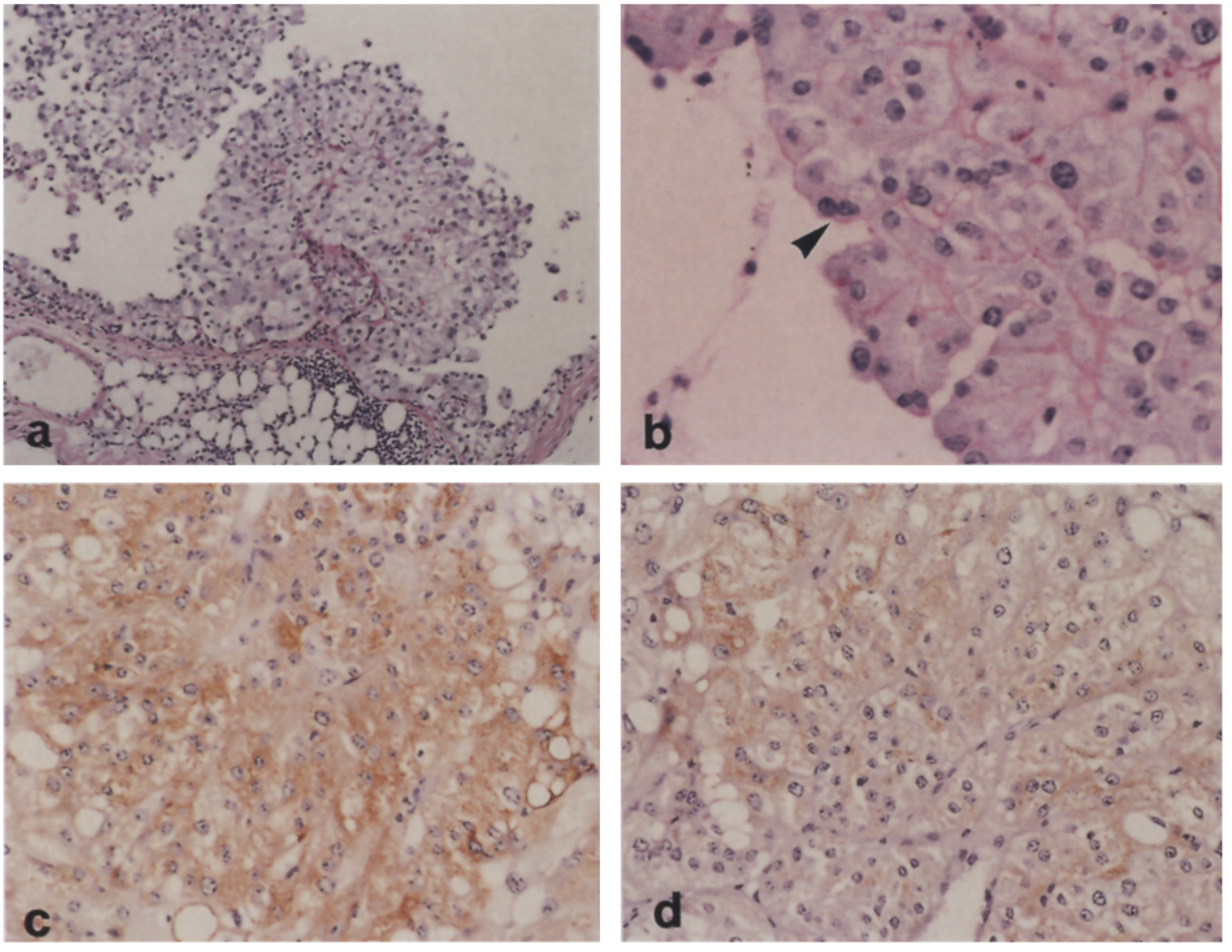

Fig. 4a–d The renal tumour from a mouse at 12 months after 4 weeks of treatment. **a** A pile up of atypical cells in the cyst wall and tumour formation with a papillary pattern are seen. (PAS, ×100). **b** Very slightly PAS-positive glycocalyx is seen on the cell surface of papillary tumours *(arrowhead).* (PAS, ×400). **c** Cystic tumours show positive reaction with DBA. (DBA, ×200). **d** Cystic tumours are partially positive for soybean agglutinin (SBA). (SBA, ×200)

Table 3 Reactivity of periodic acid-Schiff (*PAS*) stain, γ glutamyltranspeptide (*γ-GTP*) activity transforming growth factor-α (*TGF-α*) and various lectins in the renal cortical epithelial cells of untreated mice (*WGA* wheat germ agglutinin, *SBA* soybean agglutinin, *PNA* peanut agglutinin, *DBA Dolichus biflows* agglutinin, ++ strongly positive, + positive, ± weakly positive, – negative)

Epithelial cell	PAS stain	γ-GTP activity	TGF-α	Lectins			
				WGA	SBA	PNA	DBA
Bowman's capsule							
flat squamous cells	–	–	–	+	–	–	–
columnar cells	±	±	–	+	–	–	–
Proximal tubules	+	+	–	+	–	–	–
Distal tubules	–	–	+	++	± (Partial)	+	± (Partial)
Collecting ducts	–	–	++	++	+ (Partial)	+	+ (Partial)

mal tubules, but distal tubules, collecting ducts, flat cells and columnar cells of Bowmann's capsule were unstained for cold Schiff's reagent, indicating that they did not undergo lipid peroxidation (Fig. 1).

The results of PAS, γ-GTP activity, TGF-α histochemistry and lectin binding sites in the renal tubules and Bowman's capsule of untreated mouse are shown in Table 3 [4, 14]. TGF-α was detected in the brush border of proximal tubules and the cytoplasm of collecting ducts and distal tubules in an untreated mouse. Proximal tubules are characterized by the positive reaction of PAS stain, γ-GTP activity, WGA lectin stain and negative reaction of TGF-α and SBA, PNA, DBA lectin stains.

Light microscopic study in the kidney 48 h after the last Fe-NTA treatment showed many regenerative cells with large atypical nuclei. Large prominent nucleoli were often present. They had a luminal brush border that was PAS-positive (Fig. 2), and they were positive for γ-GTP activity. These karyomegalic cells were present randomly in proximal tubules including in cysts in all Fe-NTA injected animals throughout the experiments. There were a few cysts whose walls were composed of flat and squamous cells with remnants of glomeruli. They were the type 2 cysts we will describe later. No remarkable change was found in distal tubules and collecting ducts.

From 4 months from the start of treatment we observed cysts in animals of groups 1–4, irrespective of the iron dose. All cysts were located in the renal cortex and there were three identifiable types.

Type 1

The cells of the cyst wall were irregularly sized, columnar or cuboidal with eosinophilic granular cytoplasm and round large atypical nuclei situated in the center. The cell borders were usually distinct. There was a distinct PAS-positive luminal brush border and basement membrane (Fig. 3a). The luminal brush border was positive for γ-GTP activity. Those cells were positive for WGA lectin and partially positive for PNA but negative for DBA and SBA lectin stains. Papillary or multilayered growth pattern was present only in type 1 cysts (Fig. 3b). The papillary projections show positivity for WGA, and the apical areas show weak partial positivity for DBA (Fig. 3c) and SBA. Other type 1 cysts showed walls with cuboidal cells which tended to pile up from time of observation. They had a thick PAS-positive basement membrane, but a PAS-positive brush border was inconspicuous (Fig. 3d). The affinity for lectin histochemistry was similar to typical cysts of this group. This variant of cyst contained eosinophilic fluid, and Fe-positive macrophages (not shown in Figures). They were few.

Type 2

The cyst walls were composed of flat cells with indistinct nuclei. These cysts were often paired and sometimes contained remnants of glomeruli. They lacked a PAS-positive brush border (Fig. 3e) and γ-GTP activity. They showed positivity only for WGA lectin.

Type 3

These cysts were composed of columnar cells with a PAS-positive luminal brush border like type 1 cysts (Fig. 3f). They had positivity for WGA, and unlike type 1 cysts, PNA staining was negative. They had a PAS-positive basement membrane and remnants of glomeruli. In both type 2 and type 3 cysts, there were no atypical cells and papillary projections or piling up of cyst wall cells were not observed. The results of PAS staining and other histochemical studies on experimental animals are summarized in Table 4. Table 5 shows the incidence of each type of cyst including type 1 cysts with multilayered or papillary proliferation 48 h and several months after the last treatment. The number of type 1 cysts apparently increased with time. Type 3 cysts were few in number.

Thirteen-to-fifteen months after the start of the experiments, we found proliferation of atypical cells and tumour formation together with type 1 cysts. Typically, the tumour showed papillary architecture and slightly eosinophilic granular cytoplasm (Fig. 4a), and the tumour cells had a very slightly PAS-positive glycocalyx on the cell surface (Fig. 4b). We did not observe tumours composed of clear or chromophobic cells. They were positive for WGA, DBA (Fig. 4c) and partially positive for SBA (Fig. 4d). A tubular growth pattern with a luminal brush border that was slightly positive for PAS stain (Fig. 5a) was seen in part of a cystic-papillary tumour. The cytoplasm was weakly positive for γ-GTP activity (Fig. 5b),

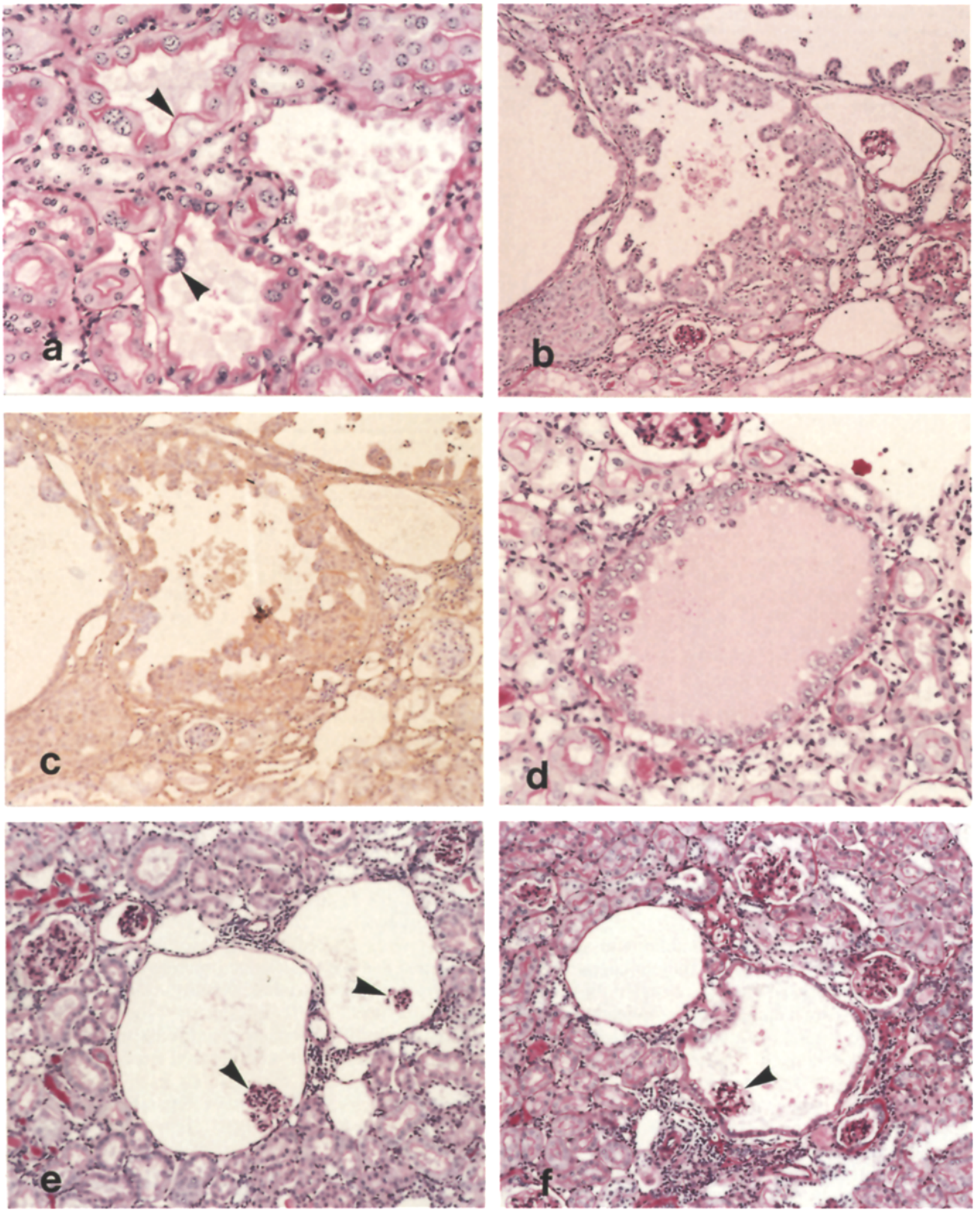

Fig. 3a–f Three types of cyst are shown. **a** A kidney section from a mouse killed 8 months after 4 weeks of Fe-NTA treatment. The tall and large atypical cells of type 1 cysts have a PAS-positive brush border *(arrowhead)*. (PAS, ×200). **b** Papillary projection is seen within the cyst. (PAS, ×100). **c** Lectin histochemistry for *Dolichos biflorus agglutinin* (DBA). The apical area of papillary projection shows the weak positivity. (DBA, ×100). **d** Another photomicrograph of the same kidney section as one in Figure 4a. The cyst is composed of multilayered cuboidal cells and has eosinophilic fluid and some inflammatory cells. (PAS, ×200). **e** Cysts are dilated and composed of flat cells, contain remnants of glomeruli *(arrowhead)* and are negative for PAS stain. (PAS, ×100). **f** This cyst is composed of PAS-positive columnar cells and also has a remnant of a glomerulus *(arrowhead)*. (PAS, ×100)

Table 4 Histochemical and immunohistochemical reaction for regenerative cells, renal cysts and tumours

	PAS stain	γ-GTP activity	TGF-α	Lectins WGA	SBA	PNA	DBA
Regenerative cells	+	+	−	+	−	−	−
Cysts: type 1	+/±	+	−	+	−	± (Apical and partial)	−
with papillary proliferation	+		−	+	± (Apical and partial)	−	± (Apical and partial)
type 2	−	−	−	+	−	−	−
type 3	+	+	−	+	−	−	−
Renal tubular tumours:	+	±	−	+	−	−	+
papillary	+	±	−	+	± (Partial)	−	+
solid	−		−	+	±	−	+

Table 5 The incidence of a various type of cysts 48 h and several months after the last Fe-NTA treatment

	Time after the last treatment			
	48 h	4 months	8 months	12 months
Type 1	0	1.8/3.5 (50%)	21/31 (70%)	18/29 (61%)
with multilayered proliferation	0	0.3/3.5 (7%)	0.7/31 (2%)	1.3/29 (5%)
with papillary proliferation	0	0	0.7/31 (2%)	0.7/29 (2%)
Type 2	3.5/3.5[a] (100%)	1.5/3.5 (43%)	7.3/31 (24%)	8/29 (28%)
Type 3	0	0	0.7/31 (2%)	1.3/29 (5%)

[a] Mean number of each cyst/mean number of all cysts observed in one kidney section (percentage)

and positive for WGA and DBA (Fig. 5c). PAS-positive glycocalyx was observed on the cell surface of all cystic-papillary tumours. Some tumours were solid with granular cells, negative for PAS stain, positive for WGA, DBA and slightly positive for SBA. All types cyst and tumours were negative for TGF-α (Table 4).

Discussion

Renal cysts develop in various conditions in humans. In acquired cystic disease of the kidney, bilateral multiple cysts are seen in atrophic kidneys in renal failure and dialysis. Such cysts are a recognized complication in dialysis patients and a series of changes from cyst, atypical epithelium and adenoma to adenocarcinoma occur with a high incidence in the same kidney [10, 19, 25]. These renal cysts and carcinomas are reported to be of proximal tubule origin based on lectin histochemistry [15, 16]. This course of tumour development cannot be followed in human sporadic renal cancer. It is suggested that the microscopic finding of cysts and tumours and cyst-tumour sequences in experimental animals is similar to those in human acquired cystic disease of the kidney [21, 24].

In experimental animals, renal cysts are often associated with the development of renal cell carcinoma. Rats fed a carcinogen such as N-(4′-fluoro-4-biphenylyl) acetamide and agricultural fungicide such as merpafol and mice injected with streptozotocin showed renal cysts before showing renal adenoma or carcinoma [7, 12, 21, 24, 33]. The results from streptozotocin-induced mice also suggested the earliest neoplastic lesion is a papillary proliferation into proximal tubules [12]. Using the renal tumour induction model by Fe-NTA in ddY mice, we followed the histogenetic cyst formation-tumour induction sequence.

A few days after Fe-NTA injection, the regenerative cells that had a PAS-positive brush border appeared (Table 4). We recognized three types of cysts several months after treatment. The findings of PAS stain, γ-GTP, TGF-α and lectin histochemistry confirmed that regenerative cells and type 1 cysts were derived from renal proximal tubules. Only type 1 cysts had atypical cells as components of the cyst wall, and showed papillary proliferation which may be a preneoplastic lesion (Table 5). We suppose that type 2 and 3 cysts originate from Bowman's capsules and have no relationship to tumours since no proliferative changes were observed. In distal tubules and collecting ducts, we did not find atypical cells or multilayered or papillary proliferation. PAS stain, γ-GTP and TGF-α histochemistry suggested cystic-papillary renal tumours were derived from papillary projection of type 1 cysts and were of proximal tubular origin. All cys-

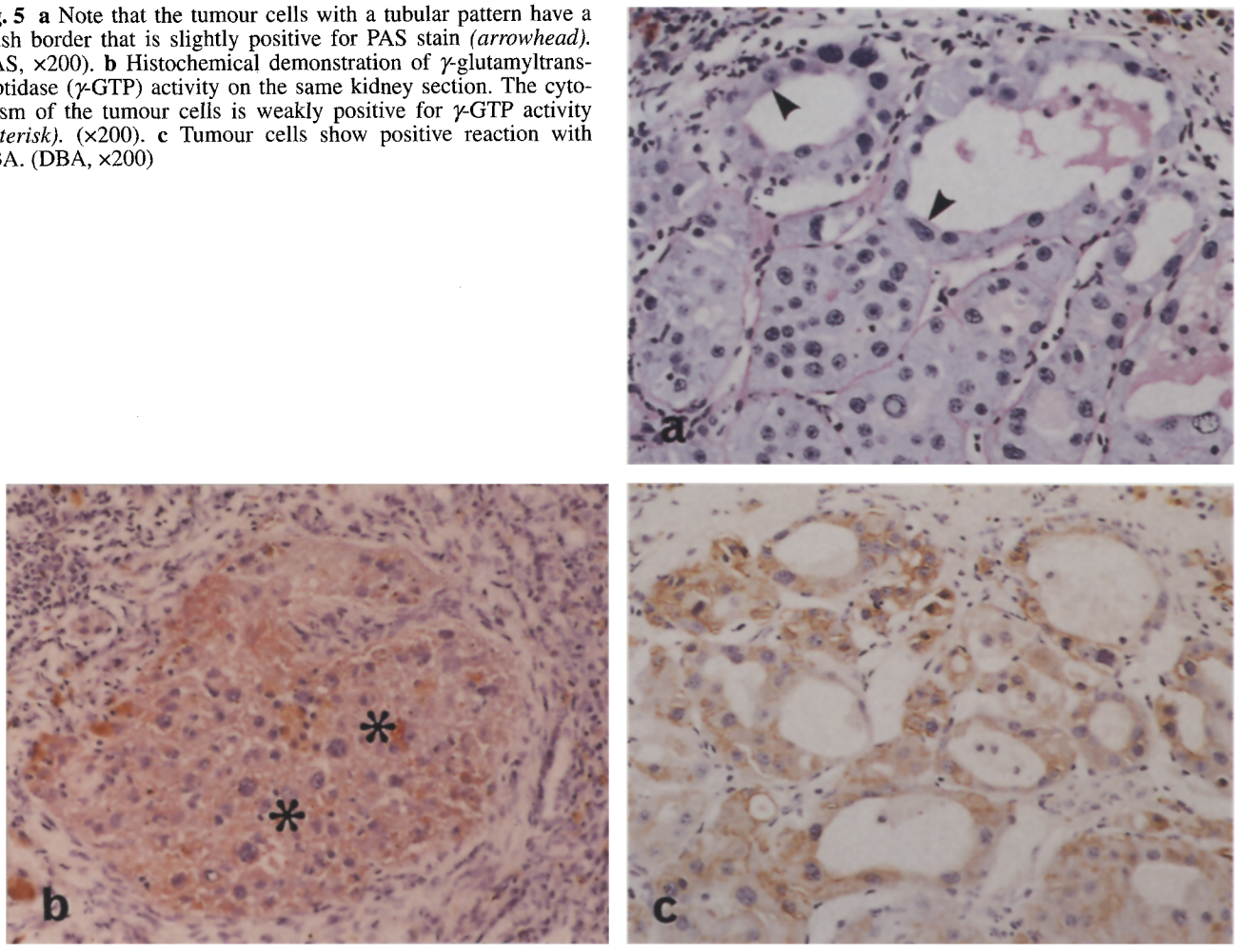

Fig. 5 **a** Note that the tumour cells with a tubular pattern have a brush border that is slightly positive for PAS stain *(arrowhead)*. (PAS, ×200). **b** Histochemical demonstration of γ-glutamyltranspeptidase (γ-GTP) activity on the same kidney section. The cytoplasm of the tumour cells is weakly positive for γ-GTP activity *(asterisk)*. (×200). **c** Tumour cells show positive reaction with DBA. (DBA, ×200)

tic-papillary tumours (73% of all tumours) were suspected to be of proximal tubular origin.

Lectin histochemistry in tumour cells showed some discrepancies, although lectins are useful in investigating the origin of cysts in human cystic kidneys [15]. Epithelial cells covering papillary projections in cysts and tumour cells showed positive reaction by SBA and DBA that are positive only in distal tubules and collecting ducts of untreated mice. Tubular and papillary lesions in tumours showed a different staining pattern for SBA (Table 4). The reason for these discrepancies is unknown. One interpretation would be that the tumours might have developed from distal tubules or collecting ducts. For example, Noguiera et al. concluded that basophilic and chromophobic renal cell tumours in rats developed from proximal tubules, whereas renal cell tumours of clear and/or acidophilic cells and oncocytomas originate in the collecting duct system [3, 22, 23]. Recently, Turusov and Chemeris used 1,2-dimethylhydrazine in CBA male mice and observed clear-cell, acidophilic or mixed tumours located in the renal cortex. Their histochemical studies showed the majority of the renal cell tumours were negative for γ-GTP staining and probably originated from the distal tubules or collecting ducts [36]. But some histochemical reactions suggested that they might arise from the proximal tubules [1]. The different methods of inducing cancer may have different target cells. In the present study, we would prefer another interpretation; namely that the binding affinity of lectins may change during the process of carcinogenesis [17]. Thus, the binding affinity of SBA and DBA in type 1 cysts is different from normal proximal tubule cells (Tables 3, 4). In a pattern consistent with our results, many renal tumours, solid or cystic, which develop in experimental animals are suspected to be of renal proximal tubular origin based on the observation of a brush border by light and electron microscopy [6, 8, 13, 21]. We could not determine the origin of our solid tumours, and have to take into consideration that they may be of distal tubule or collecting duct origin.

In normal adult male mice, high columnar cells predominate over low squamous cells in the parietal layer of Bowman's capsule [5], and they have a PAS-positive luminal brush border. Unlike the renal proximal tubule, lipid peroxidation is not observed and γ-GTP activity,

which is essential for Fe-NTA induced lipid peroxidation and necrosis [29], is low in these cells. Type 3 cysts were probably derived from these cells of Bowman's capsule, and we could not recognize any papillary change and tumour formation.

Fe-NTA is a non-genotoxic carcinogen, and administration of aluminum-NTA induces severe acute renal tubular necrosis without lipid peroxidation [27]. Repeated injection does not induce renal tumours [11]. A single injection of Fe-NTA caused lipid peroxidation and acute tubular necrosis and regenerative atypical cells appeared, but no renal tumours were seen after long-term observation (personal observation of Okada S.). We suspect that repeated injection of Fe-NTA and induction of lipid peroxidation is necessary for tumour development. The relation between Fe-NTA induced lipid peroxidation and renal tumours was recently reviewed [30].

In our previous experiment 4-week-old A/J mice were given Fe-NTA 1.8 mg–2.7 mg Fe/kg/day 6 days a week for 12 weeks to induce renal tumours [18]. We used 3-week-old male mice and injected Fe-NTA at 10 mg Fe/kg, twice a week, to maximize the amount of Fe administered and to minimize the number of animal deaths. Our data showed the injection of Fe-NTA every day for 12 weeks was not needed to induce renal tumours and that the minimum dose of Fe-NTA capable of inducing renal tumours was injection of 10 mg Fe/kg, four times in 2 weeks.

Unexpectedly, we found a much lower incidence of renal tumours in the ddY mice of group 4 (Table 2) than the A/J mice treated with Fe-NTA for 12 weeks [18]. We suppose that this was caused by the difference of animal strain used and frequency of injections, and believe that varying animal susceptibility is important, a possibility which must be taken into account in any future study of cancer induction.

Acknowledgements This work was supported by a grant-in-aid for scientific research from the Ministry of Education, Science and Culture, Japan. The authors thank Mr. H. Sakai for animal care, and Mr. Y. Arashima and Mr. H. Watanabe for their technical assistance.

References

1. Ahn Y, Chemeris G, Turusov V, Bannasch P (1994) Enzymic pattern of preneoplastic and neoplastic lesions induced in the kidney of CBA mice by 1,2-dimethylhydrazine. Toxicol Pathol 22:415–422
2. Awai M, Narasaki M, Yamanoi Y, Seno S (1979) Induction of diabetes in animals by parenteral administration of ferric nitrilotriacetate: a model of experimental hemochromatosis. Am J Pathol 95:663–674
3. Bannasch P, Zerban H (1990) Animal models and renal carcinogenesis. In: Eble J (ed) Tumors and tumor-like conditions of the kidney and ureters. Churchill Livingstone, New York, pp 4–21
4. Coppee I, Gabius HJ, Danguy A (1993) Histochemical analysis of carbohydrate moieties and sugar-specific acceptors in the kidneys of laboratory mouse and the golden spiny mouse *(Acomys russatus)*. Histol Histopathol 8:673–683
5. Crabtree C (1941) The structure of Bowman's capsule as an index of age and sex variations in normal mice. Anat Rec 79: 395–413
6. Dees JH, Reuber MD, Trump BF (1976) Adenocarcinoma of the kidney: I Ultrastructure of renal adenocarcinomas induced in rats by N-(4′-Fluoro-4-biphenylyl) acetamide. J Natl Cancer Inst 57:779–794
7. Dees JH, Heatfield BM, Reuber MD, Trump BF (1980) Adenocarcinoma of the kidney: III Histogenesis of renal adenocarcinoma induced in rats by ultrastructure of renal adenocarcinomas induced in rats by N-(4′-Fluoro-4-biphenylyl) acetamide. J Natl Cancer Inst 64:1537–1545
8. Dees JH, Heatfield BM, Trump BF (1980) Adenocarcinoma of the kidney: IV Electron microscopic study of the development of renal adenocarcinoma induced in rats by N-(4′-Fluoro-4-biphenylyl) acetamide. J Natl Cancer Inst 64:1547–1562
9. Deguchi J, Kawabata T, Kondo A, Okada S (1993) Transforming growth factor-α expression of renal proximal tubules in Wister rats treated with ferric and aluminum nitrilotriacetate. Jpn J Cancer Res 84:649–655
10. Dunnill MS, Millard PR, Oliver D (1977) Acquired cystic disease of the kidneys: a hazard of long-term intermittent maintenance haemodialysis. J Clin Pathol 30:868–877
11. Ebina Y, Okada S, Hamazaki S, Ogino F, Li JL, Midorikawa O (1986) Nephrotoxicity and renal cell carcinoma after use of iron- and aluminum-nitrilotriacetate complexes in rats. J Natl Cancer Inst 76:107–113
12. Hard GC (1985) Identification of a high-frequency model for renal carcinoma by the induction of renal tumors in the mouse with a single dose of streptozotocin. Cancer Res 45:703–708
13. Hard GC (1986) Experimental models for the sequential analysis of chemically-induced renal carcinogenesis. Toxicol Pathol 14:112–122
14. Holthöfer H (1983) Lectin binding sites in kidney, a comparative study of 14 animal species. J Histochem Cytochem 31: 531–537
15. Ishikawa I, Horiguchi T, Shikura N (1989) Lectin peroxidase conjugate reactivity in acquired cystic disease of the kidney. Nephron 51:211–214
16. Kikuchi Y (1989) Lectin and immunohistochemical studies on acquired cystic kidney and associated renal cell carcinoma. Acta Pathol Jpn 39:373–380
17. Kikuchi Y, Aizawa S, Nikaido T (1987) Lectin histochemical and immunohistochemical studies on normal kidneys and renal cell carcinoma (in Japanese). Rinsho Hinyokika 41: 951–955
18. Li JL, Okada S, Hamazaki S, Ebina Y, Midorikawa O (1987) Subacute nephrotoxicity and induction of renal cell carcinoma in mice treated with ferric nitrilotriacetate. Cancer Res 47: 1867–1869
19. Lin JI, Saklayen M, Ehrenpresis M, Hillman NM (1992) Acquired cystic disease of kidney associated with renal cell carcinoma in chronic dialysis patients. Urology 39:190–193
20. Lojda Z, Gossrau R, Stoward PJ (1991) Appendix 31 Histochemical methods for proteases. In: Stoward PJ, Pearse AGE (eds) Histochemistry, theoretical and applied. Churchill Livingstone, Edinburgh pp 639
21. Miyao N, Kumamoto Y, Tsukamoto T (1991) Histopathological analysis of chemical carcinogenesis process by streptozotocin in the mouse kidney (in Japanese). Nippon Hinyouki Gakkaishi 82:1399–1407
22. Nogueria E, Klimek F, Weber E, Bannasch P (1989) Collecting duct origin of rat renal clear cell tumors. Virchows Arch [B] 57:275–283
23. Nogueria E, Cardesa A, Mohr U (1993) Experimental models of kidney tumors. J Cancer Res Clin Oncol 119:190–198
24. Nyska A, Waner T, Pirak M, Gordon E, Bracha P, Klein B (1989) The renal carcinogenic effect of merpafol in the Fischer 344 rat. Isr J Med Sci 25:428–432
25. Ohmori, T, Sekigawa S, Sunagawa M, Tatsumi Y, Ohshima M, Enoki N, Kitahori Y, Hiasa Y, Murata Y (1981) Confirmation of the development of multiple renal cell tumors in end-

stage/long-term haemodialysis kidney revealed typical acquired cystic transformation. Acta Pathol Jpn 31:1097–1104
26. Okada S, Midorikawa O (1982) Induction of the rat renal adenocarcinoma by Fe-nitrilotriacetate (Fe-NTA) (in Japanese). Naika Houkan (Jpn Arch Int Med) 29:485–491
27. Okada S, Hamazaki S, Ebina Y, Li JL, Midorikawa O (1987) Nephrotoxicity and its prevention by vitamin E in ferric nitrilotriacetate-promoted lipid peroxidation. Biochim Biophys Acta 922:28–33
28. Okada S, Fukunaga Y, Hamazaki S, Yamada Y, Toyokuni S (1991) Sex differences in the localization and severity of ferric nitrilotriacetate-induced lipid peroxidation in the mouse kidney. Acta Pathol Jpn 41:221–226
29. Okada S, Minamiyama Y, Hamazaki S, Toyokuni S, Sotomatsu A (1993) Glutathione cycle dependency of ferric nitrilotriacetate-induced lipid peroxidation in mouse proximal renal tubules. Arch Biochem Biophys 301:138–142
30. Okada S, Hamazaki S, Akiyama T, Liu M (in press) Iron-induced carcinogenesis in experimental animals: a free radical mechanism of DNA damage and carcinogenesis. In: Cutler R, Packer L, Mori A (eds) Oxidative Stress and Aging. Birkhäuser, Basel
31. Pompella A, Maellaro E, Casini AF, Comporti M (1987) Histochemical detection of lipid peroxidation in the liver of bromobenzene-poisoned mice. Am J Pathol 129:295–301
32. Rutenberg AM, Kim H, Fischbein JW, Hanker JS, Wasserkrug HL, Seligman AM (1968) Histochemical and ultrastructural demonstration of γ-glutamyl transpeptidase activity. J Histochem Cytochem 17:517–526
33. Shinohara Y, Frith C (1980) Morphologic characteristics of benign and malignant renal cell tumors in control and 2-acetylaminofluorene-treated BALB/c female mice. Am J Pathol 100:455–468
34. Spater HW, Poruchynsky MS, Quintana N, Inoue M, Novikoff AB (1982) Immunocytochemical localization of γ-glutamyltransferase in rat kidney with protein A-horseradish peroxidase. Proc Natl Acad Sci USA 79:3547–3550
35. Toyokuni S, Okada S, Hamazaki S, Minamiyama Y, Yamada Y, Liang P, Fukunaga Y, Midorikawa O (1990) Combined histochemical and biochemical analysis of sex hormone dependence of ferric nitrilotriacetate-induced renal lipid peroxidation in ddY mice. Cancer Res 50:5574–5580
36. Turusov VS, Chemeris GY (1992) Renal cell tumors induced in CBA male mice by 1,2-dimethylhydrazine. Toxicol Pathol 20:570–575
37. Wachstein M (1955) Histochemical staining of the normally functioning and abnormal kidney. J Histochem Cytochem 3: 246–270
38. Walker C, Everitt J, Freed JJ, Kundson AG, Whiteley LO (1991) Altered expression of Transforming Growth Factor-α in hereditary rat renal cell carcinoma. Cancer Res 51: 2973–2978